



Calhoun: The NPS Institutional Archive

Theses and Dissertations

Thesis Collection

1960

Spectral analysis of 500-mb pressure-height data

LeDew, Thomas A.

Monterey, California. Naval Postgraduate School

<http://hdl.handle.net/10945/13083>



Calhoun is a project of the Dudley Knox Library at NPS, furthering the precepts and goals of open government and government transparency. All information contained herein has been approved for release by the NPS Public Affairs Officer.

Dudley Knox Library / Naval Postgraduate School
411 Dyer Road / 1 University Circle
Monterey, California USA 93943

<http://www.nps.edu/library>

NPS ARCHIVE
1960
LEDEW, T.

SPECTRAL ANALYSIS OF 500-MB
PRESSURE-HEIGHT DATA

THOMAS A. LE DEW
and
ROBERT E. MELHORN

Library
U. S. Naval Postgraduate School
Monterey, California

**DUDLEY KNOX LIBRARY
NAVAL POSTGRADUATE SCHOOL
MONTEREY, CA 93943-5101**

DUDLEY KNOX LIBRARY
NAVAL POSTGRADUATE SCHOOL
MONTEREY, CA 93943-5101

5
SPECTRAL ANALYSIS OF 500-mb PRESSURE-HEIGHT DATA

Thomas A. LeDew

Robert E. Melhorn

SPECTRAL ANALYSIS OF 500-mb PRESSURE-HEIGHT DATA

5

by

Thomas A. LeDew, Lieutenant, U. S. Navy
//

and

Robert E. Melhorn, Lieutenant, U. S. Navy

Submitted in partial fulfillment of the
requirements for the degree of

MASTER OF SCIENCE

IN

METEOROLOGY

United States Naval Postgraduate School
Monterey, California

1960

WPS ARCHIVE

1960

LEDEW, T.

SPECTRAL ANALYSIS OF 500-mb PRESSURE-HEIGHT DATA

by

Thomas A. LeDew

and

Robert E. Melhorn

This work is accepted as fulfilling the
thesis requirements for the degree of

MASTER OF SCIENCE

IN

METEOROLOGY

from the

United States Naval Postgraduate School

DUDLEY KNOX LIBRARY
NAVAL POSTGRADUATE SCHOOL
MONTEREY, CA 93943-5101

ABSTRACT

Distributions of kinetic energy by latitude and wave number were obtained from harmonic analyses of hemispherical weather charts. Correlations between daily changes in these kinetic energies were also computed.

The writers wish to express their gratitude to Professor George J. Haltiner, U. S. Naval Postgraduate School, and Commander Paul Wolff, Officer-in-charge of NANWEP, for their suggestion of the topic and continued assistance and encouragement.

TABLE OF CONTENTS

Section	Title	Page
1	Introduction	1
2	Development of kinetic energy equations	2
3	Correlation coefficients	5
4	Kinetic energy distribution	6
5	Correlation of kinetic energy changes	11
6	Conclusions	16
7	Recommendations	18
8	Illustrations	19

LIST OF ILLUSTRATIONS

Figure	Title	Page
1	Total KE(U), total KE(u), total KE(v), and total E	19
2	KE(u) and KE(v) vs n for 17 ⁰ .5N.	19
3	KE(u) and KE(v) vs n for 22 ⁰ .5N.	20
4	KE(u) and KE(v) vs n for 27 ⁰ .5N.	20
5	KE(u) and KE(v) vs n for 32 ⁰ .5N.	21
6	KE(u) and KE(v) vs n for 37 ⁰ .5N.	21
7	KE(u) and KE(v) vs n for 42 ⁰ .5N.	22
8	KE(u) and KE(v) vs n for 47 ⁰ .5N.	22
9	KE(u) and KE(v) vs n for 52 ⁰ .5N.	23
10	KE(u) and KE(v) vs n for 57 ⁰ .5N.	23
11	KE(u) and KE(v) vs n for 62 ⁰ .5N.	24
12	KE(u) and KE(v) vs n for 67 ⁰ .5N.	24
13	E and E per unit area vs \emptyset	25
14	KE(U) and KE(u) \neq KE(v) all n vs \emptyset	25
15	KE(u) all n vs \emptyset	26
16	KE(v) all n vs \emptyset	26
17	KE(v) all n vs \emptyset , different scale	26
18	KE(u) and KE(v) n = 1 vs \emptyset	27
19	KE(u) and KE(v) n = 2 vs \emptyset	27
20	KE(u) and KE(v) n = 3 vs \emptyset	27
21	KE(u) and KE(v) n = 4 vs \emptyset	27
22	KE(u) and KE(v) n = 5 vs \emptyset	28
23	KE(u) and KE(v) n = 6 vs \emptyset	28
24	KE(u) and KE(v) n = 7 vs \emptyset	28

Figure	Title	Page
25	KE(u) and KE(v) $n = 8$ vs \emptyset	28
26	KE(u) $n = 9$ vs \emptyset	29
27	KE(u) $n = 10$ vs \emptyset	29
28	KE(u) $n = 11$ vs \emptyset	29
29	KE(u) $n = 12$ vs \emptyset	29
30	KE(v) $n = 1$ vs \emptyset	30
31	KE(v) $n = 2$ vs \emptyset	30
32	KE(v) $n = 3$ vs \emptyset	30
33	KE(v) $n = 4$ vs \emptyset	30
34	KE(v) $n = 5$ vs \emptyset	31
35	KE(v) $n = 6$ vs \emptyset	31
36	KE(v) $n = 7$ vs \emptyset	31
37	KE(v) $n = 8$ vs \emptyset	31
38	KE(v) $n = 9$ vs \emptyset	32
39	KE(v) $n = 10$ vs \emptyset	32
40	KE(v) $n = 11$ vs \emptyset	32
41	KE(v) $n = 12$ vs \emptyset	32

1. Introduction

In the Monthly Weather Review of July 1958, Commander Paul Wolff, U. S. Navy, prescribed a method for improving numerical weather forecasts. His development decreased the errors due to faulty prediction of the movements of very long wave components of the pressure patterns. At the conclusion of his article, Commander Wolff suggested that empirical methods currently employed could be replaced by terms in equations describing the mechanism by which energy is transferred to and from long waves.

The purposes of this paper are to show the distribution of kinetic energy by latitude and wave number and to correlate daily changes in the kinetic energy of various wave numbers and latitudes with one another.

For this research, data for 120 days during the winter of 1947-48 were used. These data, furnished by the NAVAL WEATHER RESEARCH FACILITY, consisted of mean 500-mb heights for each latitude at 5° intervals from 15° N. to 70° N., as well as amplitudes and phase angles for wave numbers 1 through 18 for these latitudes. Because of time restrictions, wave numbers 13 through 18 were neglected in our computations.

2. Development of Kinetic Energy Equations

Fourier series were employed to represent the height of the 500-mb surface in order to investigate the distribution of kinetic energy. The form used for each latitude was

$$z = \bar{z} + z' \quad (1)$$

where

$$z' = \sum_{n=1}^{n=12} A_n \cos n(\theta + \delta_n)$$

z = height of 500-mb surface

\bar{z} = mean height of 500-mb surface

A_n = amplitude of wave number n

δ_n = phase angle in radians with respect to Greenwich meridian

θ = longitude in radians

The quantities z , \bar{z} , A_n , and δ_n are all functions of latitude.

Since wind data are relatively scarce, especially over oceans, the geostrophic approximation was used to obtain the wind velocity. In accordance with this approximation, the wind components may be written as

(2)

$$U = - \frac{g}{f} \frac{1}{a} \frac{\partial \bar{z}}{\partial \phi}$$

$$u = - \frac{g}{f} \frac{1}{a} \frac{\partial z'}{\partial \phi}$$

$$v = \frac{g}{f} \frac{1}{a \cos \phi} \frac{\partial z'}{\partial \theta}$$

where

$U + u$ = total zonal component of the wind velocity

v = meridional component of the wind velocity

ϕ = latitude in radians

$g =$ gravity

$a =$ radius of earth

The kinetic energies per unit mass of the mean zonal flow, the zonal perturbation wind component, and the meridional wind component are $1/2 U^2$, $1/2 u^2$, and $1/2 v^2$.

Utilizing equations (1) and (2), we obtain

$$1/2 U^2 = \left(\frac{g}{2a \sin \phi} \right)^2 \frac{1}{a^2} \left(\frac{\partial \bar{z}}{\partial \phi} \right)^2 \quad (3)$$

$$1/2 u^2 = \frac{1}{2} \left(\frac{g}{2a \sin \phi} \right)^2 \frac{1}{a^2} \left[\sum_{n=1}^{n=1/2} \frac{\partial A_n}{\partial \phi} \cos n(\theta + \delta_n) + n A_n \frac{\partial \delta_n}{\partial \phi} \sin n(\theta + \delta_n) \right]^2$$

$$1/2 v^2 = \frac{1}{2} \left(\frac{g}{2a \sin \phi} \right)^2 \frac{1}{a^2 \cos^2 \phi} \left[\sum_{n=1}^{n=1/2} n A_n \sin n(\theta + \delta_n) \right]^2$$

Multiplying by $\rho a \cos \phi \delta \phi$ and integrating equations (3) from 0 to 2π , we obtain kinetic energies per unit cross-section area for the latitude circle. Since the variation of the density is negligible compared to velocity, a mean value of density will be assumed.

The resulting kinetic energies expressed in terms of finite differences are as follows:

$$\begin{aligned} & \pi \rho \left(\frac{g}{2a} \right)^2 \frac{1}{a} \frac{\cos \bar{\phi}}{\sin^2 \bar{\phi}} \frac{(\bar{z}_2 - \bar{z}_1)^2}{(\pi/36)^2} \\ & \pi \rho \left(\frac{g}{2a} \right)^2 \frac{1}{a} \frac{\cos \bar{\phi}}{\sin^2 \bar{\phi}} \sum_{n=1}^{n=1/2} \left[\frac{(A_{n2} - A_{n1})^2}{(\pi/36)^2} + \left(\frac{A_{n1} + A_{n2}}{2} \right)^2 n^2 \frac{(\delta_{n2} - \delta_{n1})^2}{(\pi/36)^2} \right] \\ & \pi \rho \left(\frac{g}{2a} \right)^2 \frac{1}{a} \frac{\cos \bar{\phi}}{\sin^2 \bar{\phi}} \sum_{n=1}^{n=1/2} \left[\frac{n}{2} (A_{n1} + A_{n2}) / \cos \bar{\phi} \right]^2 \end{aligned}$$

where

Subscripts 1 and 2 refer to two adjacent latitude bands.

$$\bar{\phi} = 1/2 (\phi_1 + \phi_2)$$

$$\bar{z} = \text{mean height}$$

$$\pi/36 = \text{latitudinal increment}$$

A common factor has been omitted and values quoted subsequently are relative kinetic energies. To obtain values of the kinetic

energies in cgs units, it is merely necessary to multiply the relative kinetic energies by 0.145×10^6 . The following quantities have been evaluated on the CDC Model 1604 computer for the relative kinetic energies of the mean zonal flow and the perturbation components for each wave number:

$$KE(U) = k(\phi) \left(\bar{u}_2 - \bar{u}_1 \right)^2 / \left(\pi/36 \right)^2$$

$$KE(u) = k(\phi) \left[\left(A_{n_2} - A_{n_1} \right)^2 + n^2 \left(\frac{A_{n_1} + A_{n_2}}{2} \right)^2 \left(\delta_2 - \delta_1 \right)^2 \right] / \left(\pi/36 \right)^2$$

$$KE(v) = k(\phi) \left[n(A_{n_2} - A_{n_1}) \right]^2 / \cos^2 \bar{\phi}$$

where

$$k(\phi) = \cos \bar{\phi} / \sin^2 \bar{\phi}$$

3. Correlation Coefficients

Correlation coefficients were computed between the daily changes in relative kinetic energy of each component originally calculated, as well as the sums of these components for each wave number and each latitude band. Again the Control Data Corporation Model 1604 computer was utilized because of its high speed and large memory capacity.

The product-moment correlation coefficient, r , for relating two variables x and y was employed.

$$r = \text{covariance } (x,y) / \sigma_x \sigma_y$$

where

$$\text{covariance } (x,y) = \frac{1}{n} \sum x_i y_i - \bar{x} \bar{y}$$

$$\sigma_x = \sqrt{\frac{1}{n} \sum x_i^2 - \bar{x}^2}$$

$$\sigma_y = \sqrt{\frac{1}{n} \sum y_i^2 - \bar{y}^2}$$

4. Kinetic energy distribution

In order to appreciate the energy distribution presented below, it must be remembered that the kinetic energy was computed using the geostrophic approximation of the real wind, which is not entirely valid, especially at very low latitudes. The latitude range considered is from 15°N . to 70°N . The daily kinetic energies for the 120 days were computed for eleven latitude bands, each 5° in width. The units used here are arbitrary and do not represent absolute values, but illustrate the relative magnitudes of the various components of kinetic energy as they are distributed geographically. In order to yield absolute kinetic energy in cgs units, the relative magnitudes must be multiplied by a factor of 0.145×10^6 . Occasionally, the scale on certain graphs is changed to emphasize salient features. A note to this effect is addended so that an erroneous conception of relative magnitudes will be avoided.

The following notation was used in the preparation of figures.

E = total kinetic energy

$KE(U)$ = mean zonal kinetic energy

$KE(u)$ = zonal component of the perturbation kinetic energy
for each wave number

$KE(v)$ = meridional component of the perturbation kinetic
energy for each wave number

n = wave number

ϕ = latitude

The wave numbers, n , range from 1 through 12, and the latitude bands discussed are represented by mean latitudes of the bands as follows:

$\phi_1 = 17^{\circ}.5N$	$\phi_2 = 22^{\circ}.5N$	$\phi_3 = 27^{\circ}.5N$
$\phi_4 = 32^{\circ}.5N$	$\phi_5 = 37^{\circ}.5N$	$\phi_6 = 42^{\circ}.5N$
$\phi_7 = 47^{\circ}.5N$	$\phi_8 = 52^{\circ}.5N$	$\phi_9 = 57^{\circ}.5N$
$\phi_{10} = 62^{\circ}.5N$	$\phi_{11} = 67^{\circ}.5N$	

Figure 1 illustrates the hemispheric distribution of total kinetic

energy at 500 mb over the latitudes of $15^{\circ}N$. through $70^{\circ}N$. The total kinetic energy, E , is composed of total mean zonal kinetic energy, $KE(U)$, total zonal component of the perturbation kinetic energy, $KE(u)$, and total meridional component of the perturbation kinetic energy, $KE(v)$.

It is seen from this figure that the mean zonal contribution is slightly less than the $KE(u)$ contribution. Of the perturbation components, the contribution of the zonal perturbation, $KE(u)$, is about three times as great as the meridional perturbation, $KE(v)$.

Figures 2-12 depict the relative magnitudes of $KE(u)$ and $KE(v)$ contributions of wave numbers 1 through 12. Each figure represents the spectrum at a given latitude band. It should be noted that these spectra are discrete and have meaning only for integral values of wave number. The lines connecting points have been drawn to aid visual tracing of fluctuations. Also note that the mean zonal contribution, $KE(U)$, is not dependent on wave number.

In summary of figures 2-12, we note several significant features. Notably, the spectra reveal that at very low latitudes the maximum kinetic energy is contained in wave number 2 of the $KE(u)$ component, corresponding to a very long wave length of 180° longitude. The maximum in the $KE(u)$ component shifts toward higher wave number as latitude is increased, until, at $42^{\circ}.5N$, wave number 4 is a maximum contributor. This indicates that the largest single contribution of

kinetic energy at this particular middle latitude is associated with a wave length of 90° . The maximum shifts back to wave number 2 as latitude is further increased, although wave number 4 continues to be significant. Above wave number 7 the KE(u) component is relatively small at all latitudes.

The KE(v) contribution is comparatively small at lower latitudes, but begins to become significant above $42^\circ.5N$. At these higher latitudes, the KE(v) contribution is insignificant in wave number 1, but compares in magnitude to the KE(u) in higher wave numbers and contributes more to the total energy.

The profile of the total kinetic energy, E, is as depicted in figure 13. The initially high value of kinetic energy at ϕ_1 is undoubtedly a reflection of the trades. The minimum at ϕ_2 corresponds to the winter position of the subtropical high pressure belt near $22^\circ.5N$. The maximum at ϕ_3 shows the latitudinal position of the westerly jet to be around $37^\circ.5N$. Again it must be noted that the values at the various latitude bands are discrete. The values of total kinetic energy decrease steadily as latitude increases northward of $37^\circ.5N$. This is partially a result of the decrease of the area of a latitudinal band approaching the pole. The dotted line in figure 13 shows the total kinetic energy per unit area. It is apparent that the kinetic energy decrease at high latitudes is therefore primarily a reflection of a decreased wind intensity.

The contribution of KE(U) is small at latitudes above ϕ_3 , but contributes significantly to the total kinetic energy at lower latitudes except at the subtropical high pressure belt, ϕ_2 . (See figure 14).

The profile of the total $KE(u)$, figure 15, illustrates an overall decrease with increasing latitude above ϕ_2 , whereas the total $KE(v)$ given in figure 16, increases up to ϕ_7 and then decreases. The $KE(v)$ profile is also shown with the magnitude scale expanded in figure 17 to emphasize the latitudinal distribution of $KE(v)$.

The spectra of perturbation kinetic energy are shown in figures 2-12. It should be noted that the maximum energy is located at ϕ_1 for $n = 2$, as seen in figure 2, followed by a secondary maximum at ϕ_5 for $n = 4$, as seen in figure 7. The profiles are fairly uniform at $n = 4$ and above, indicating a consistent distribution for the higher wave numbers. The very long waves, $n = 1, 2, 3$, have higher values at low latitudes and a somewhat erratic distribution. One conclusion that may be drawn from this set of graphs is that the long waves, 1-3, contribute most of the kinetic energy at ϕ_2 . Figure 14 shows that this contribution is largely due to the perturbation kinetic energy.

Figures 18-41 show the spectra of perturbation kinetic energy contributions. Note that an enlarged scale is used beginning with figure 30 for the $KE(v)$ profiles.

In discussing the total zonal perturbation and mean zonal kinetic energy contributions, it was pointed out that these components comprised the greatest part of the total kinetic energy in the longer waves ($n = 1-6$) at the lower latitudes (ϕ_8 and below). The $KE(v)$ contribution is not significant below ϕ_8 . It was also pointed out that perturbation kinetic energy is not particularly significant at any of the latitudes under consideration in short waves ($n = 7-12$). Therefore, in discussing the perturbation profiles we shall confine

ourselves to low wave numbers. Figure 18 shows that the $KE(v)$ contribution is negligible for $n = 1$. Figure 30 shows this component with an enlarged magnitude scale. Although the value of $KE(v)$ for $n = 1$ increases with latitude, it is two orders of magnitude smaller than the corresponding $KE(u)$. Figures 19-25 show that the $KE(v)$ contribution approaches and sometimes equals the $KE(u)$ contribution at high latitudes for wave numbers 2-8.

The $KE(v)$ components are expanded in figures 30-41, as a matter of interest, to show the latitudinal distribution of this relatively small contributor to the total kinetic energy.

5. Correlation of Kinetic Energy Changes

The correlation of 24-hour kinetic energy changes over the 120-day data period was made complete as practicable with the aid of the CDC Model 1604 computer. The following items were correlated with one another:

1. Changes in total kinetic energy (all wave numbers, all latitudes).
2. Changes in total kinetic energy at each latitude for all wave numbers.
3. Changes in total kinetic energy for each wave number over all latitudes.
4. Changes in total kinetic energy at each latitude for each wave number.
5. Changes in total mean zonal kinetic energy (all latitudes).
6. Changes in total mean zonal kinetic energy at each latitude.
7. Changes in total zonal perturbation kinetic energy (all wave numbers, all latitudes).
8. Changes in zonal perturbation kinetic energy at each latitude for all wave numbers.
9. Changes in zonal perturbation kinetic energy in each wave number over all latitudes.
10. Changes in total meridional perturbation kinetic energy (all wave numbers, all latitudes).
11. Changes in meridional perturbation kinetic energy at each latitude for all wave numbers.
12. Changes in meridional perturbation kinetic energy in each wave number over all latitudes.

The program was designed to extract only correlation coefficients equal to or greater than 0.4. A large number of high positive correlation coefficients was obtained, but time limitations have prevented a complete analysis of the results. The complete printout of the correlation coefficients with instructions and identifier table for locating the items correlated will be left with Professor George Haltiner, U. S. Naval Postgraduate School, Monterey, California.

Twenty-two negative correlation coefficients in the range, -0.40 to -0.47, were obtained and these are presented in Table I below. It was felt that a negative correlation of kinetic energy changes would better indicate the existence of kinetic energy transfer relationships. The notation is the same as that used in Section 4 with the addition of the symbols \sum^{ϕ} , \sum^n , which represent the sum of the indicated kinetic energy component over all latitudes and all wave numbers, respectively.

Inspection of these correlations shows the existence of change in the total meridional perturbation component at latitude $47^{\circ}5N$. occurring simultaneously with an opposite change in the (1) mean zonal component, (2) total zonal perturbation component, and (3) total kinetic energy at latitude $22^{\circ}5N$. This negative correlation between the total meridional component at $47^{\circ}5N$. and the total kinetic energy at $22^{\circ}5N$. is a result of the negative correlations between the former and total kinetic energy changes in all wave numbers except $n = 2$ and $n = 5$.

It is of interest that latitude $22^{\circ}5N$. approximately corresponds to the position of the subtropical high pressure belt during the winter months, whereas latitude $47^{\circ}5N$. corresponds to the position of the

polar front. At the 500-mb level, which approximates the level of non-divergence, the average vertical air mass transport at $47^{\circ}5N$. would be upward, whereas at $22^{\circ}5N$. it would be downward.

TABLE I

$\sum_{n=1}^{11} KE(v)$ at $47^{\circ}.5$ vs $KE(u)$ at $17^{\circ}.5$ for $n = 3$

$\sum_{n=1}^{11} KE(v)$ at $47^{\circ}.5$ vs $KE(u)$ at $22^{\circ}.5$

$\sum_{n=1}^{11} KE(v)$ at $47^{\circ}.5$ vs $KE(v)$ at $22^{\circ}.5$ for $n = 3$

$\sum_{n=1}^{11} KE(v)$ at $47^{\circ}.5$ vs E at $22^{\circ}.5$ for $n = 1$

$\sum_{n=1}^{11} KE(v)$ at $47^{\circ}.5$ vs E at $22^{\circ}.5$ for $n = 3$

$\sum_{n=1}^{11} KE(v)$ at $47^{\circ}.5$ vs E at $22^{\circ}.5$ for $n = 4$

$\sum_{n=1}^{11} KE(v)$ at $47^{\circ}.5$ vs E at $22^{\circ}.5$ for $n = 6$

$\sum_{n=1}^{11} KE(v)$ at $47^{\circ}.5$ vs E at $22^{\circ}.5$ for $n = 7$

$\sum_{n=1}^{11} KE(v)$ at $47^{\circ}.5$ vs E at $22^{\circ}.5$ for $n = 8$

$\sum_{n=1}^{11} KE(v)$ at $47^{\circ}.5$ vs E at $22^{\circ}.5$ for $n = 9$

$\sum_{n=1}^{11} KE(v)$ at $47^{\circ}.5$ vs E at $22^{\circ}.5$ for $n = 10$

$\sum_{n=1}^{11} KE(v)$ at $47^{\circ}.5$ vs E at $22^{\circ}.5$ for $n = 11$

$\sum_{n=1}^{11} KE(v)$ at $47^{\circ}.5$ vs E at $22^{\circ}.5$ for $n = 12$

$\sum_{n=1}^{11} KE(v)$ at $47^{\circ}.5$ vs $\sum_{n=1}^{11} KE(u)$ at $22^{\circ}.5$

$\sum_{n=1}^{11} KE(v)$ at $47^{\circ}.5$ vs $\sum_{n=1}^{11} E$ at $22^{\circ}.5$

$\sum_{n=1}^{11} KE(v)$ at $47^{\circ}.5$ vs $KE(u)$ at $57^{\circ}.5$ for $n = 1$

$KE(v)$ at $32^{\circ}.5$ for $n = 4$ vs $KE(u)$ at $32^{\circ}.5$ for $n = 10$

$KE(v)$ at $32^{\circ}.5$ for $n = 4$ vs $KE(u)$ at $27^{\circ}.5$ for $n = 10$

$KE(v)$ at $32^{\circ}.5$ for $n = 4$ vs $\sum_{n=1}^{\phi} KE(u)$ for $n = 10$

$KE(v)$ at $32^{\circ}.5$ for $n = 4$ vs $KE(u)$ at $32^{\circ}.55$ for $n = 7$

$KE(u)$ at $27^{\circ}.5$ for $n = 4$ vs $KE(u)$ at $37^{\circ}.5$ for $n = 3$

$KE(u)$ at $22^{\circ}.5$ for $n = 6$ vs E at $47^{\circ}.5$ for $n = 12$

Between these latitudes there is a net air mass transport southward above 500 mb and a net transport northward below 500 mb. With the meridional circulation pattern in mind, it is reasonable to

assume that there is a kinetic energy interchange between these latitude belts. Figure 17 shows that the maximum in the latitudinal distribution of the total meridional kinetic energy component exists at latitude 47.5° N. It is our conjecture that changes in the total meridional perturbation kinetic energy component in the region of the polar front are caused by, or result in, opposite changes in the total kinetic energy in the belt of the subtropical high.

The negative correlation between the changes in the meridional perturbation component in $n = 4$ at latitude 32.5° N. and the changes in the zonal perturbation component in $n = 7$ at the same latitude suggest a possible energy exchange between these different wave numbers. The negative correlation between the changes in zonal perturbation components at latitude 27.5° N. in $n = 4$ and latitude 37.5° N. for $n = 3$ indicates not only an interchange between wave numbers but a possible latitudinal interchange. The negative correlations between components in the higher wave numbers would not contribute appreciably to the total kinetic energy changes at 500 mb.

6. Conclusions

In summary of the kinetic energy distributions, it is seen that total kinetic energy is high in the trades region, low in the belt of subtropical high pressure, a maximum at mid-latitudes near the westerly jet, and thereafter decreasing to a minimum approaching the pole.

The mean zonal kinetic energy contribution is greatest at mid-latitudes with a secondary maximum at the trades, and minima in the doldrums and high latitudes. Approximately half of the total hemispheric kinetic energy at 500 mb is associated with the mean zonal wind.

The rest of the total kinetic energy is perturbation kinetic energy, which resides for the most part in the longer waves, $n = 1-7$. Both the zonal and meridional components vary with wave number as shown earlier. At low latitudes only the zonal perturbation component is significant. At high latitudes, the meridional perturbation component becomes almost as important as the zonal, except for wave number 1. With these points in mind, treating both components of perturbation kinetic energy together, we see that wave number 2 contains the maximum perturbation kinetic energy at low latitudes. As latitude is increased the maximum shifts from $n = 2$ to $n = 4$ at mid-latitude, $47^{\circ}5$ N. Above this latitude the perturbation contribution at wave number 2 becomes equal to and then greater than that at $n = 4$. This is not to imply that these wave numbers are the only significant ones, they are merely the largest. The combined contributions to the total kinetic energy from the other wave numbers far outweigh the effect of these single maxima.

On the basis of the few negative correlations considered, it is seen that exchanges of kinetic energy exist between different wave

numbers at the same latitude and between various wave numbers at different latitudes. A more detailed quantitative study of these interchanges should prove very useful.

7. Recommendations

A complete analysis of the positive correlation coefficients computed for the daily changes in kinetic energy is recommended as a future investigation.

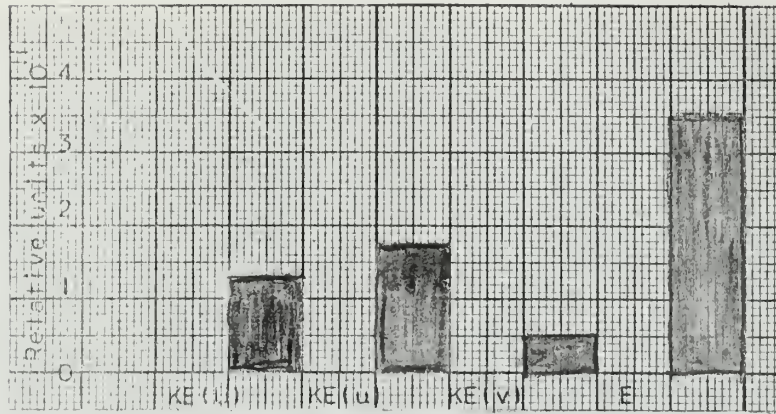


Figure 1

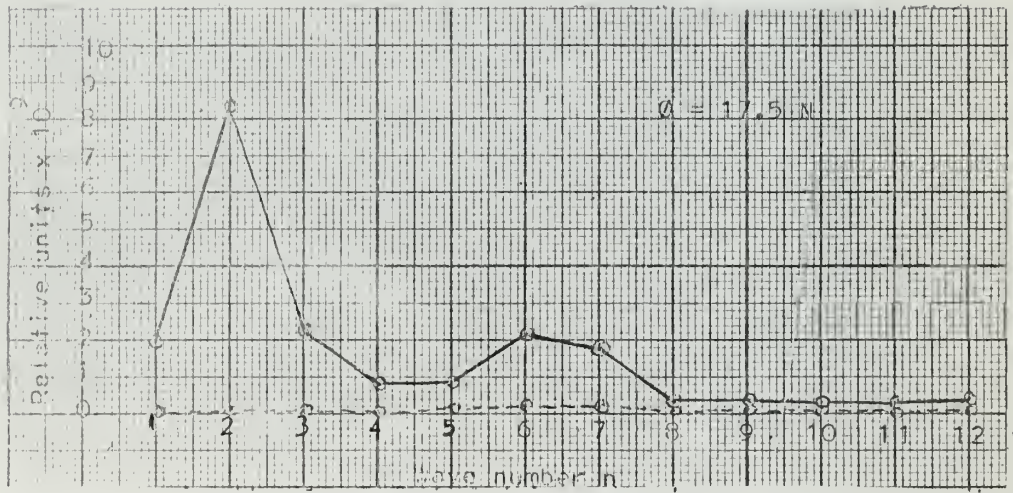


Figure 2



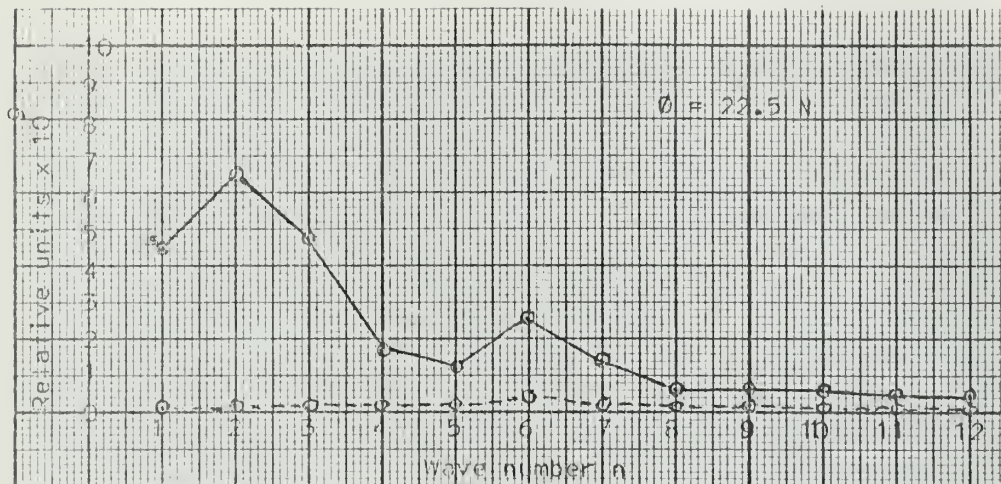


Figure 3

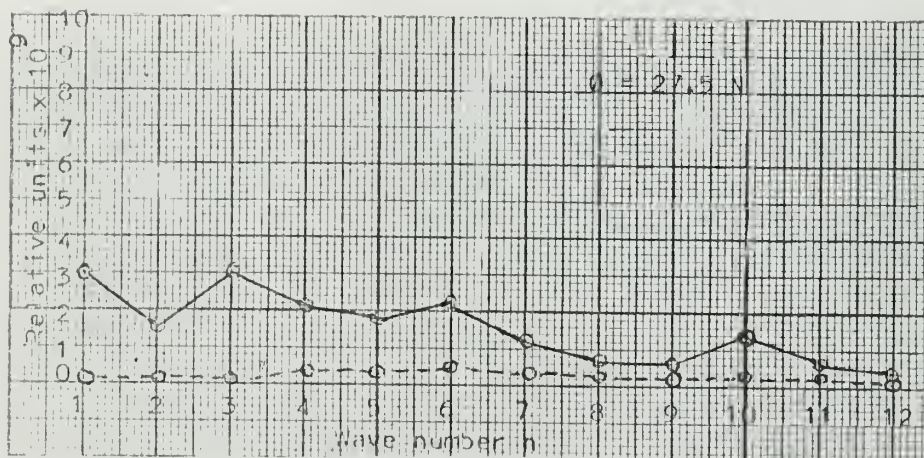


Figure 4

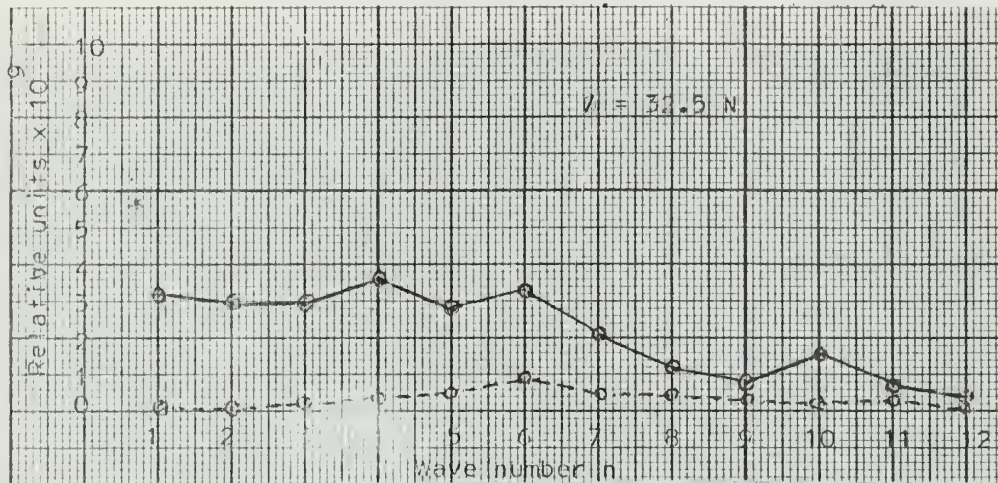


Figure 5

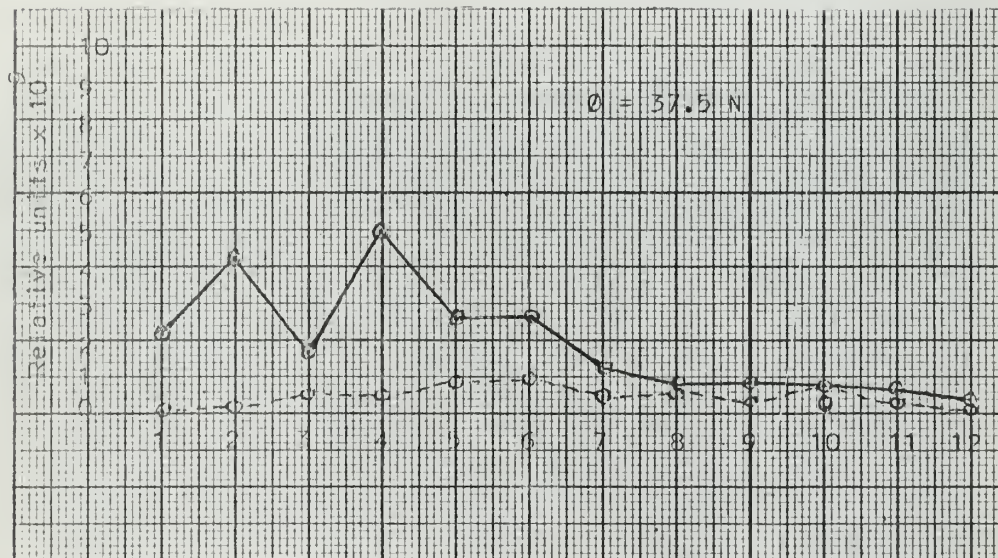


Figure 6

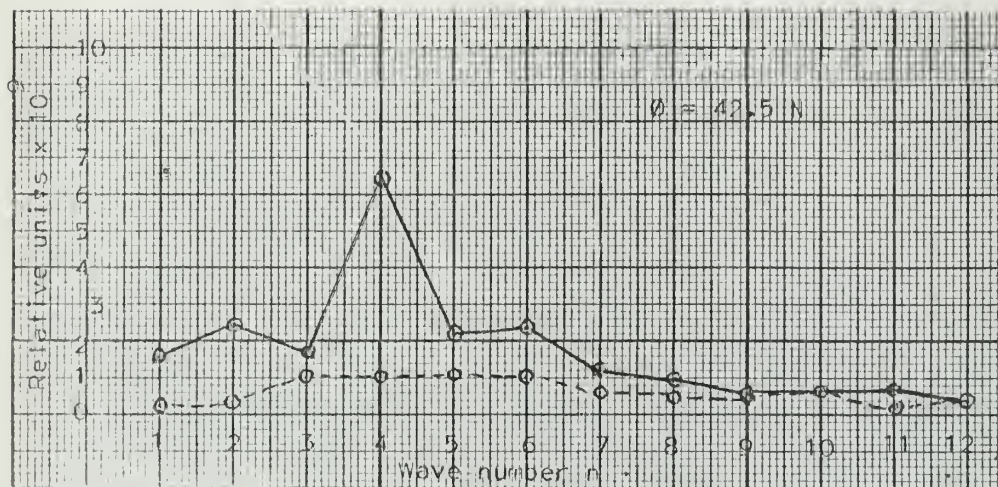


Figure 7

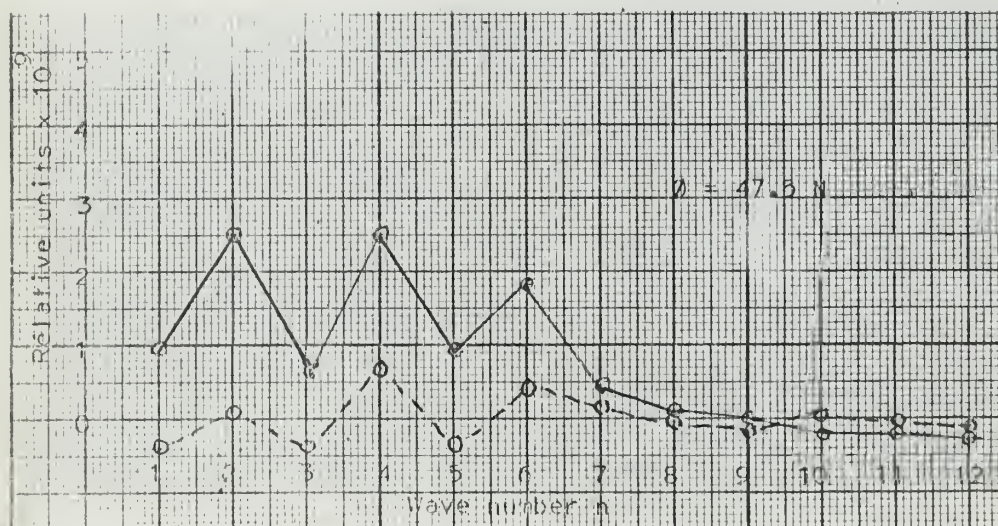


Figure 8

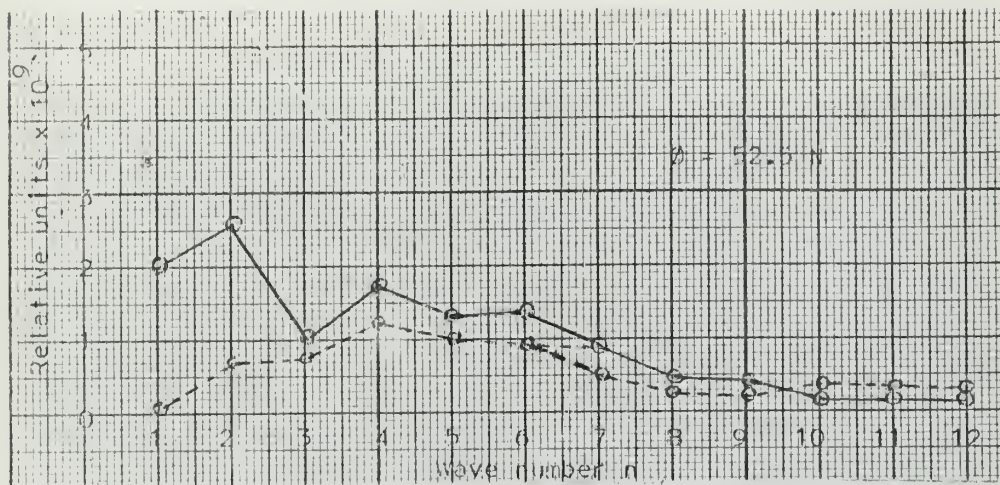


Figure 9

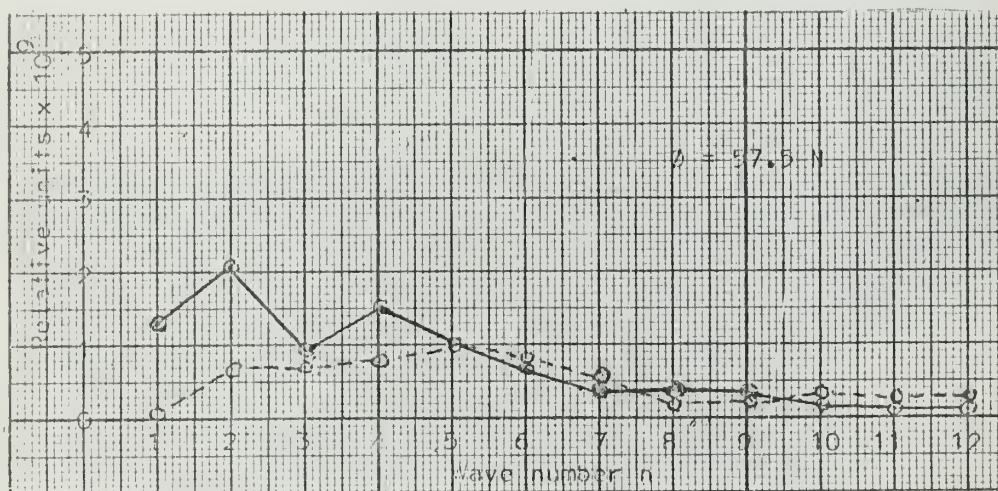


Figure 10

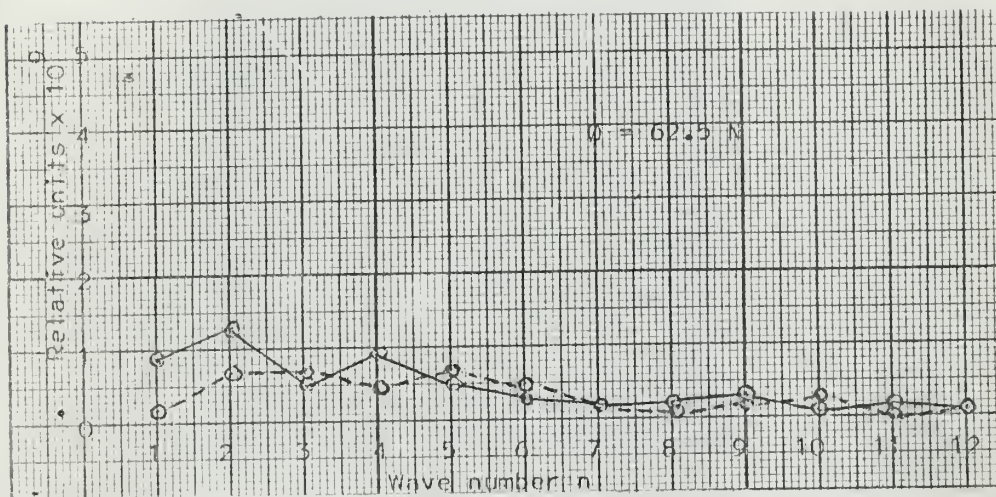


Figure 11

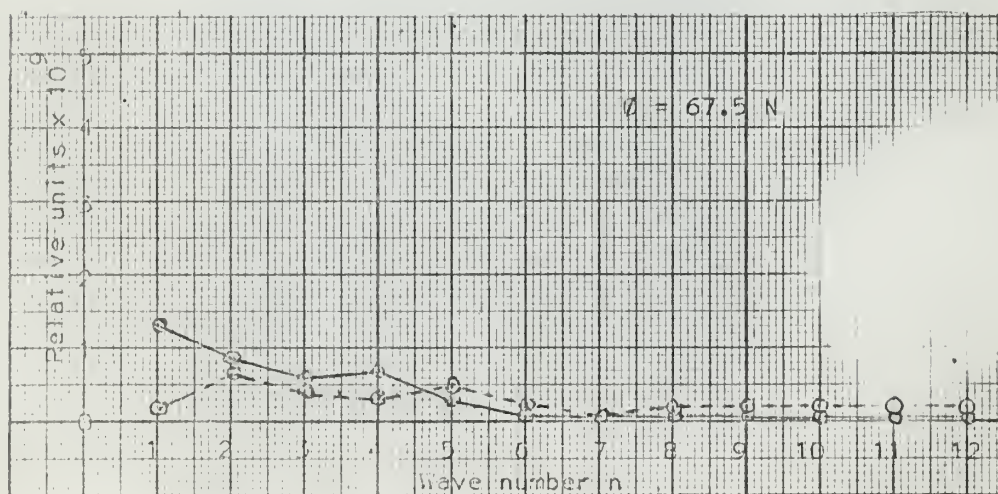


Figure 12

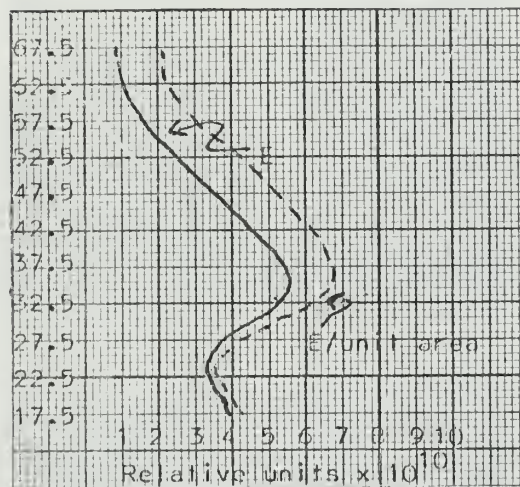


Figure 13

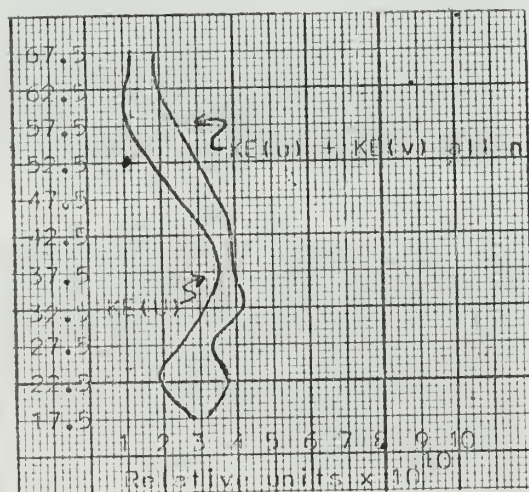


Figure 14

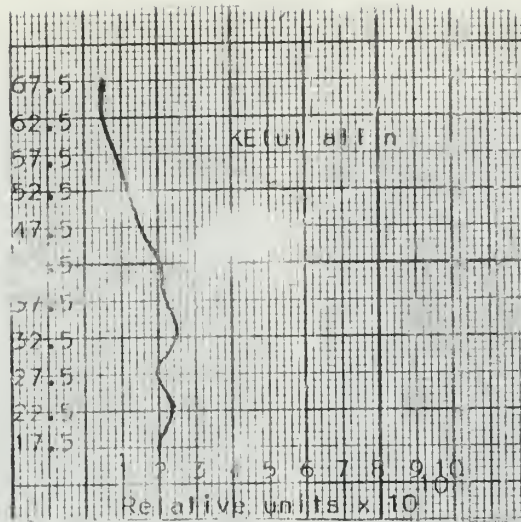


Figure 15

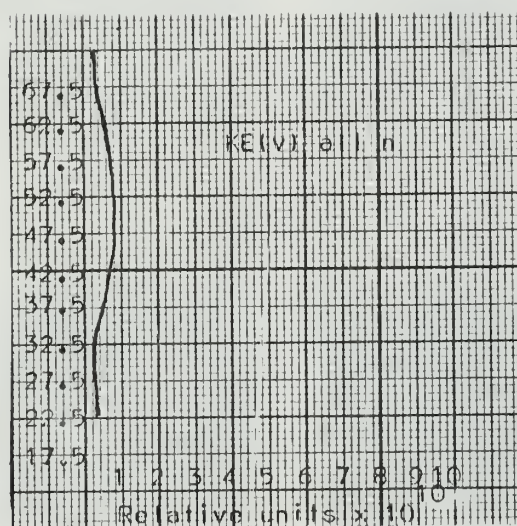


Figure 16

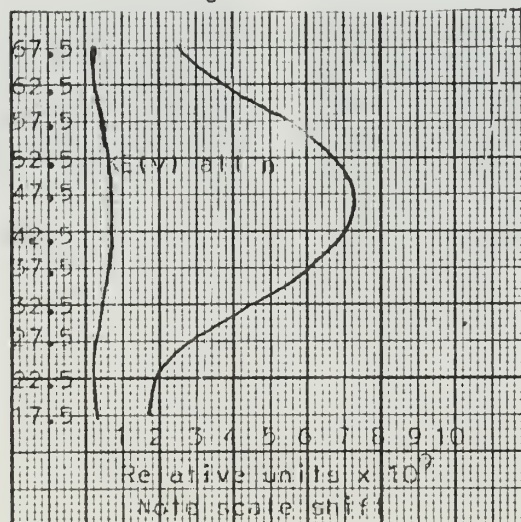


Figure 17

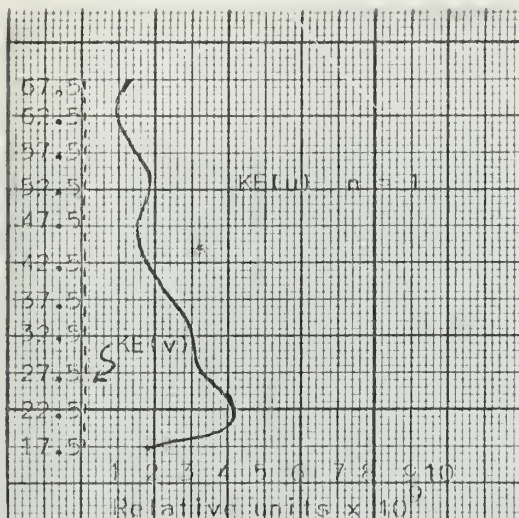


Figure 18

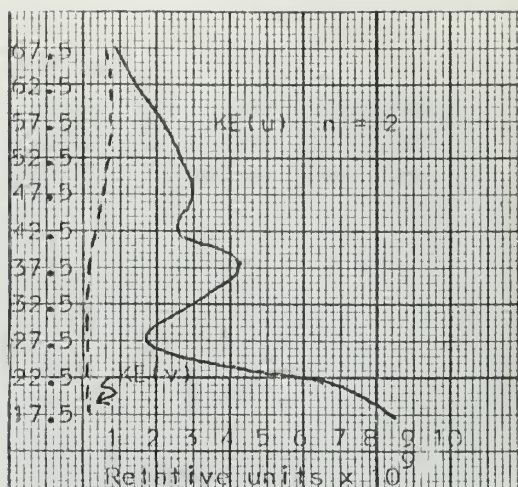


Figure 19

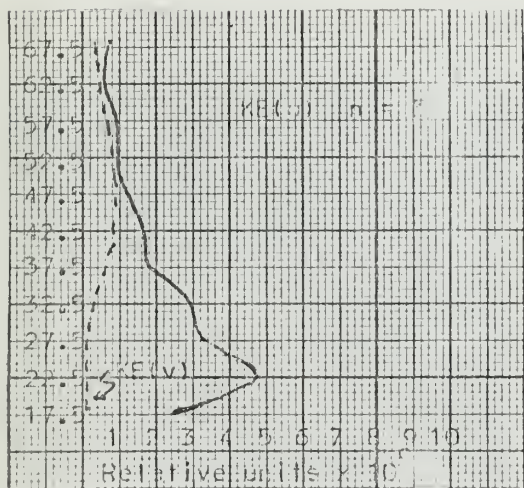


Figure 20

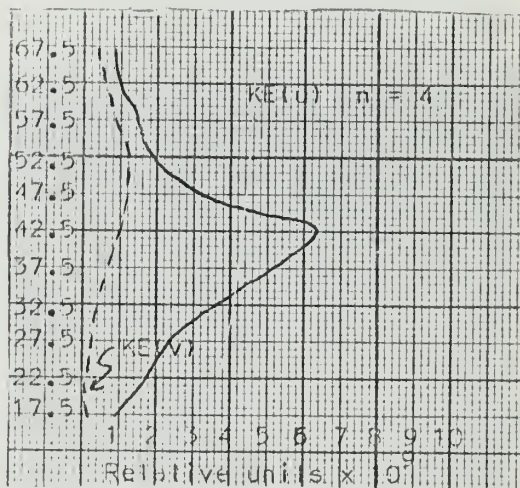


Figure 21

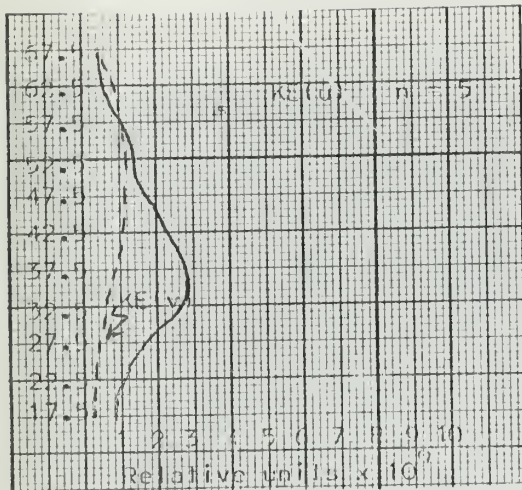


Figure 22

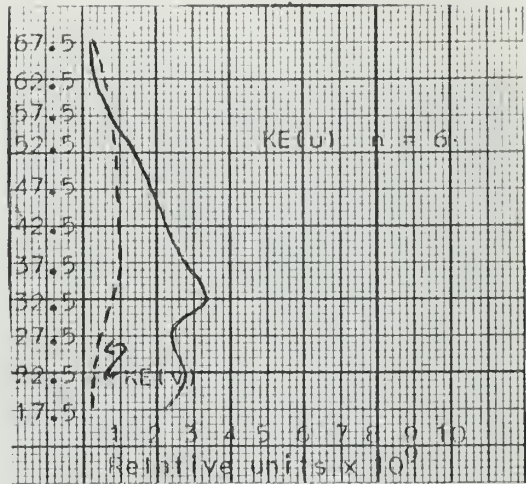


Figure 23

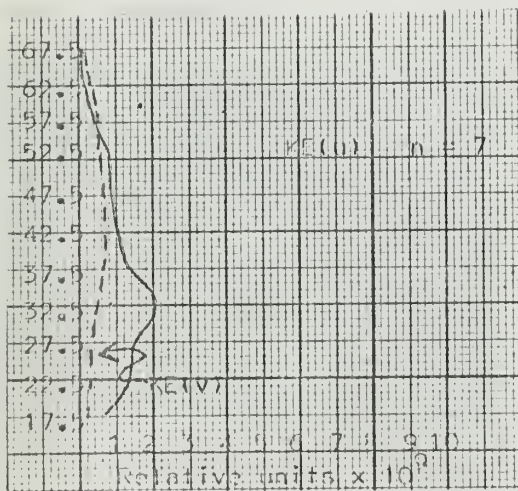


Figure 24

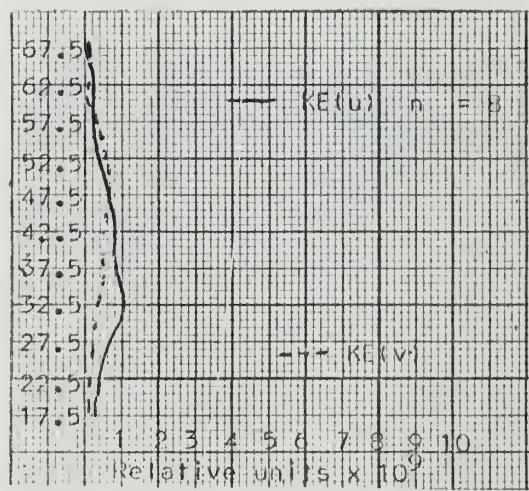


Figure 25

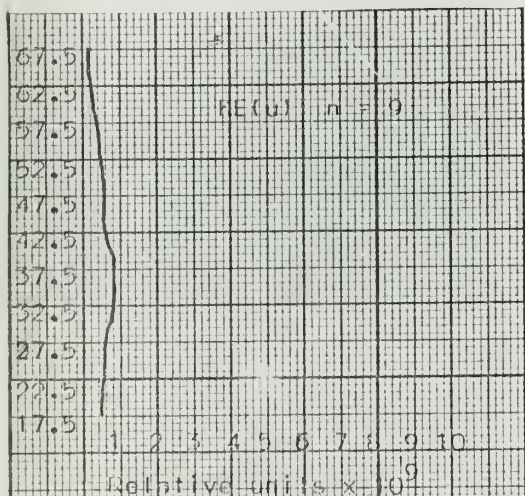


Figure 26

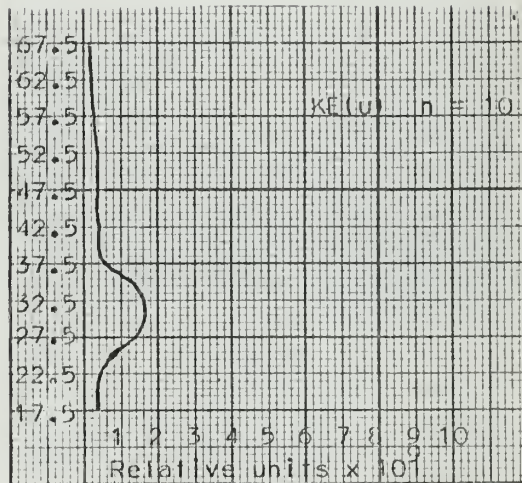


Figure 27

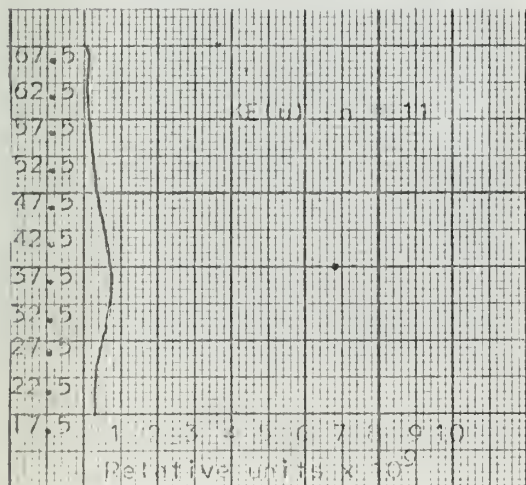


Figure 28

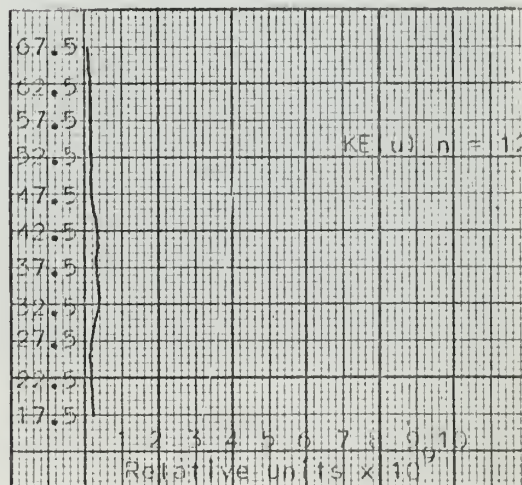


Figure 29

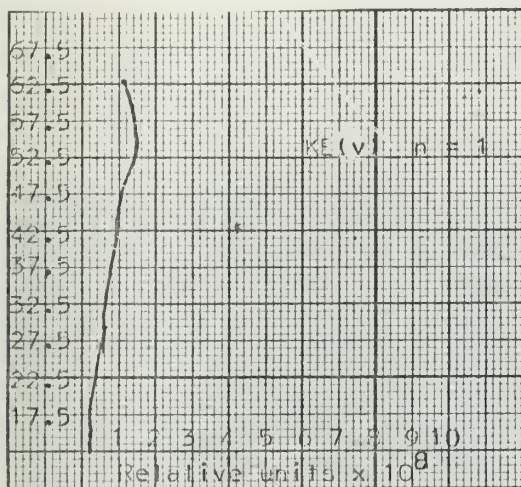


Figure 30

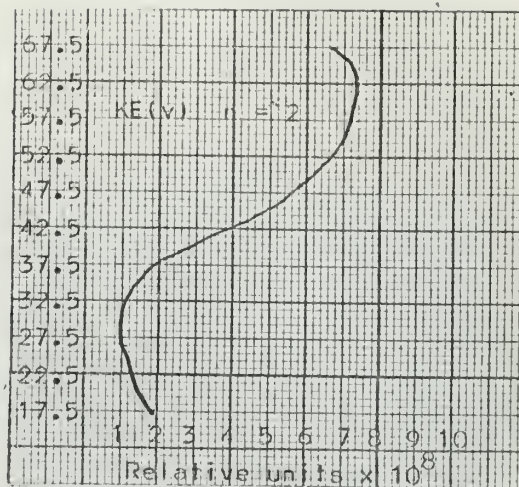


Figure 31

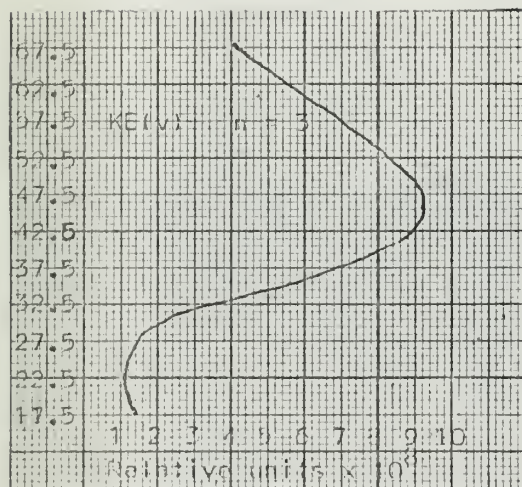


Figure 32

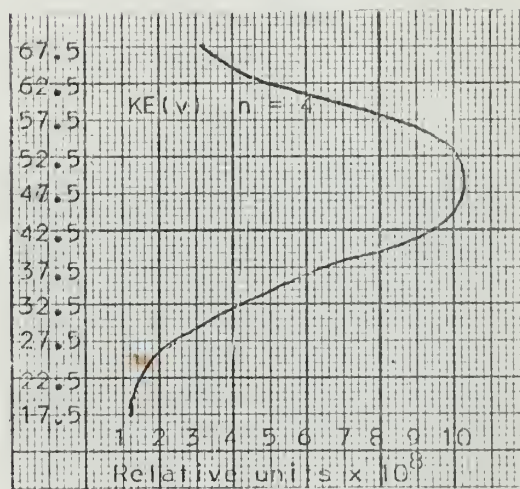


Figure 33

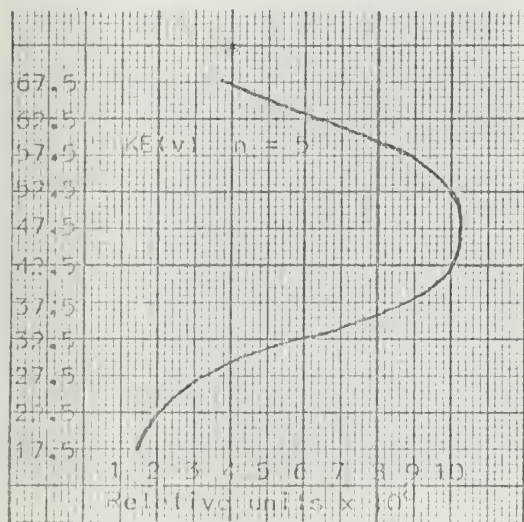


Figure 34

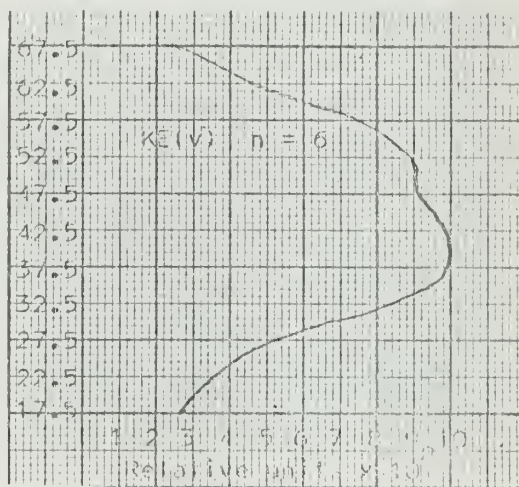


Figure 35

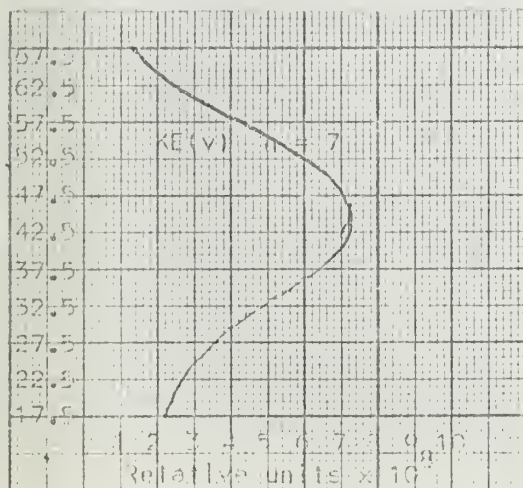


Figure 36

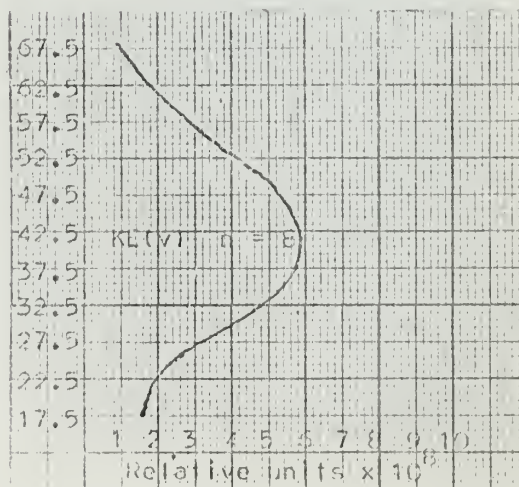


Figure 37

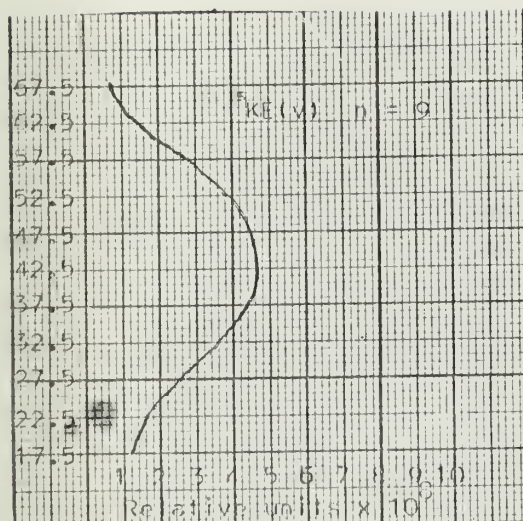


Figure 38

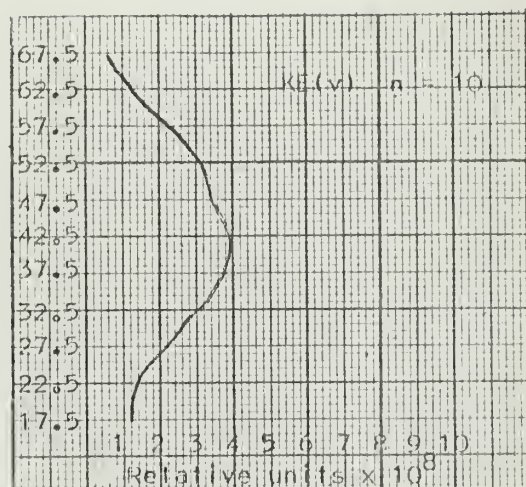


Figure 39

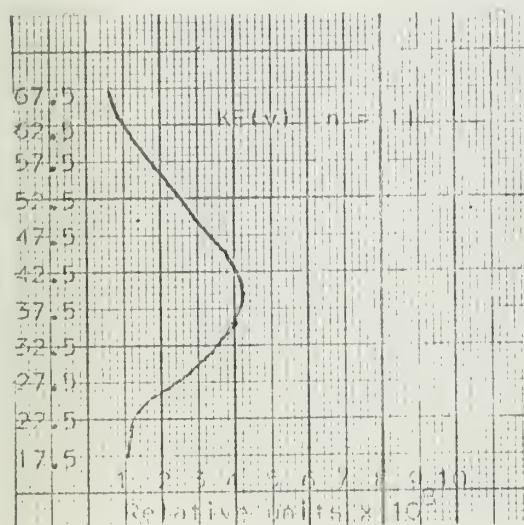


Figure 40

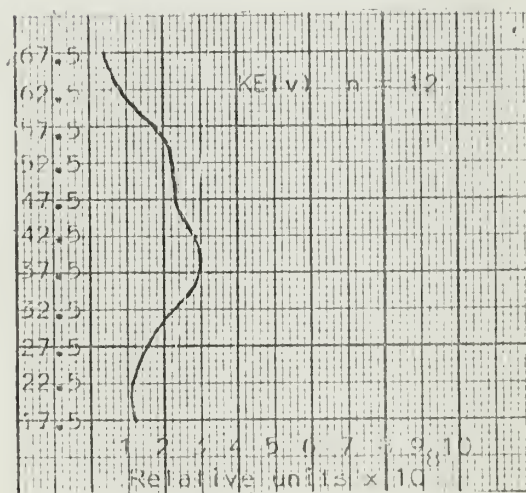
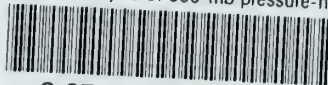


Figure 41

thesL37

Spectral analysis of 500-mb pressure-hei



3 2768 002 11986 9

DUDLEY KNOX LIBRARY